International Scholars Journals

African Journal of Physics Vol. 3 (5), pp. 119-126, May, 2016. Available online at www.internationalscholarsjournals.org © International Scholars Journals

Full Length Research Paper

Natural convection flow of a non-Newtonian Casson fluid past a vertical stretching plane with mass transfer

Gamal T. ElBaradei

Department of Mathematics, Faculty of Science, South Valley University, Qena, Egypt. E-mail: elbarad@yahoo.com.

Accepted 22 March, 2015

Three dimensional natural convection heat transfer flow of a non-Newtonian Casson fluid from a vertical stretching plane with surface mass transfer is investigated. Casson fluid model is used to characterize the non-Newtonian fluid behavior. The transformed governing nonlinear boundary layer equations are solved numerically by means of very robust computer algebra software MATLAB employing the routine bvpc45. Numerical calculations are obtained for the heat transfer from the stretching sheet and the wall temperature for a Casson parameter and a large range of values of the Prandtl number Pr . A comprehensive numerical computation is carried out for various values of the parameters that describe the flow characteristics, and the results are reported graphically. The missing values of the velocity and thermal functions are tabulated. The effect of increasing values of the Casson parameter b is to suppress the velocity field, whereas the temperature is enhanced with increasing Casson parameter.

Key words: Stretching plane, Casson fluid, free convection, mass transfer.

INTRODUCTION

Due to the numerous applications in industrial manufacturing processes, the problem of flow and heat transfer due to stretching surfaces has attracted the attention of researchers being a subject of considerable interest in the contemporary literature, [Crane, 1970; Banks, 1983; Grubka and Bobba, 1985; Magyari and Keller, 2000; Liao and Pop, 2004]. Processes involving the effects of mass transfer have attracted the attention of researchers due to its applications in many engineering applications, such as chemical processing equipments. The driving force for mass transfer is the difference in concentration. There are some fluids which react chemically with some ingredients present in them. The boundary-layer flows of non-Newtonian fluids have been given considerable attention due to ever increasing engineering applications. In order to obtain a thorough cognition of non-Newtonian fluids and their various applications, it is necessary to study their flow behaviors. It is well known that the mechanics of non-Newtonian fluids present a special challenge to engineers, physicists and mathematicians. The non-linearity can manifest itself in a variety of ways in many fields, such as food processing, drilling operations and bio-engineering.

On the other hand, the most popular among these fluids is the Casson fluid. We can define a Casson fluid as a shear thinning liquid which is assumed to have an infinite viscosity at zero rate of shear, a yield stress below which no flow occurs and a zero viscosity at an infinite rate of shear. The Casson model is a well-known rheological model for describing the non-Newtonian flow behavior of fluids with a yield stress [Casson, 1959]. The model was developed for viscous suspensions of cylindrical particles [Reher et al., 1969]. Regardless of the form or type of suspension, some fluids are particularly

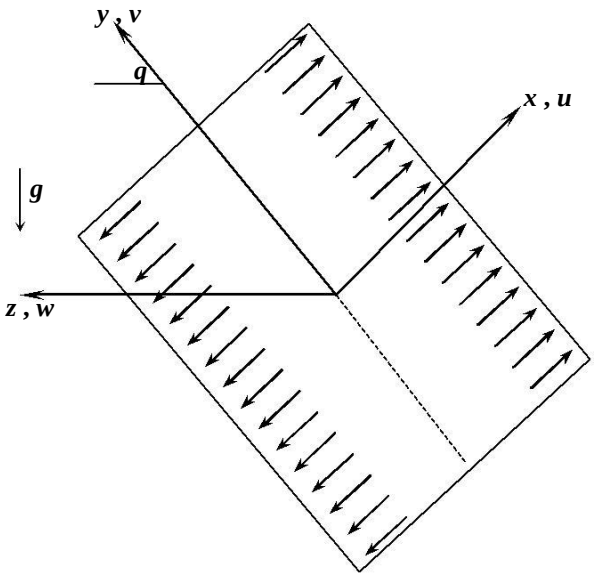

Figure 1. Coordinate system and physical model.

well described by this model because of their nonlinear yield-stress-pseudoplastic nature. Examples are blood by CoKelet et al. [1963], chocolate by Chevalley [1991] and xanthan gum solutions by Garcia-Ochoa and Casas [1994]. The Casson model fits the flow data better than the more general Herschel–Bulkley model [Remizov, 1999; Joye, 1998], which is a power-law formulation with yield stress [Bird et al., 1960; Wilkinson, 1960]. For chocolate and blood, the Casson model is the preferred rheological model. It seems increasingly that the Casson model fits the nonlinear behavior of yield-stress-pseudoplastic fluids rather well and it has therefore gained in popularity since its introduction in 1959. It is relatively simple to use, and it is closely related to the Bingham model [Bird et al., 1960; Wilkinson, 1960], which is very widely used to describe the flow of slurries, suspensions, sludge, and other rheologically complex fluids [Churchill, 1988]. Eldabe and Salwa [1995] studied the Casson fluid for the flow between two rotating cylinders. Boyd et al. [2007] investigated the Casson fluid flow for the steady and oscillatory blood flow. Boundary layer flow of Casson fluid over different geometries is considered by many authors in recent years. Nadeem et al. [2012] presented MHD flow of a Casson fluid over an exponentially shrinking sheet. Kumari et al. [2011] analyzed peristaltic pumping of a MHD Casson fluid in an inclined channel. Mukhopadhyay et al. [2013] studied the unsteady two-dimensional flow of a non-Newtonian fluid over a stretching surface having a prescribed surface temperature, the Casson fluid model is used to characterize the non-Newtonian fluid behavior. The details of steady, fully-developed and laminar flow of Casson fluids have been described in [Fung, 1981]. In view of the non-Newtonian nature of blood in capillaries and the filtration/absorption property of the walls while Oka [1979] studied blood flow in capillaries with permeable walls using the Casson fluid model. In this contribution the boundary layer flow due to stretching plane with mass transfer is studied. More studies have been obtained see Nadeem et al. [2013] and Nadeem et al., [2014a, b, c]. We venture further in the regime of three-dimensional flows of a non-Newtonian fluid. Casson fluid model is used to characterize the non-Newtonian fluid behavior.

Problem formulation

Consider a steady three-dimensional, boundary layer, non-Newtonian Casson fluid flow past a surface in the vertical plane stretching in the x –direction with a velocity bx . The y –direction makes an angle q with the horizontal line. In addition, z –direction is normal to the sheet. Casson fluid model is used to characterize the non-Newtonian fluid behavior, the physical model and coordinate system is shown in Figure 1. Assuming that the edge effects are negligible, all variables will be independent of the y –direction Moreover, the rheological equation of state for an isotropic and incompressible flow of a Casson fluid as [Eldabe and Salwa, 1995].

$$t_{ij} = \begin{cases} \left(2\mu_B + \dfrac{P_y}{\sqrt{2\pi}}\right)e_{ij}, & \pi > \pi_c \\ \left(2\mu_B + \dfrac{P_y}{\sqrt{2\pi_c}}\right)e_{ij}, & \pi < \pi_c \end{cases}$$

Where, t_{ij} is the (i, j) -th component of the stress tensor, $t_{ij} = e_{ij} e_{ij}$ and e_{ij} are the (i, j) -th component of the deformation rate, p is the product of the component of deformation rate with itself, p_c is a critical value of this product based on the non-Newtonian model, μ_B is plastic dynamic viscosity of the non-Newtonian fluid, and P_y is the yield stress of the fluid. So, if a shear stress less than the yield stress are applied to the fluid, it behaves like a solid, whereas if a shear stress greater than yield stress is applied, it starts to move. Considering the balance laws of mass, linear momentum and energy and using the Boussinesq's approximation the governing equations of this flow can be written in the usual form as:

$$\frac{\partial u}{\partial x} + \frac{\partial w}{\partial z} = 0 \qquad (1)$$

$$\frac{\partial u}{\partial x} \quad \frac{\partial u}{\partial z} \quad \left(\frac{1}{b}\right)\frac{\partial^2 u}{\partial z^2} \quad \% \qquad (2)$$

$$\frac{\partial v}{\partial z} \quad \left(\frac{1}{b}\right)\frac{\partial^2 v}{\partial z^2} \quad \% \qquad (3)$$

$$\frac{\partial w}{\partial z} = -\frac{1}{\rho}\frac{\partial P}{\partial z} + \left(\frac{1}{b}+1\right)\frac{\partial^2 w}{\partial z^2} \quad (4)$$

$$w\frac{\partial T}{\partial z} = \frac{n}{\Pr}\frac{\partial^2 T}{\partial z^2} \quad (5)$$

The appropriate boundary conditions for the governing equations are:

$$z = 0,\quad u = u_w(x) = bx,\quad v = 0,\quad w = W,\quad T = T_w$$
$$z \to \infty,\ u \to 0,\ v \to 0,\quad \frac{\partial w}{\partial z} \to 0,\quad T \to T_\infty \quad (6)$$

Where, (u, v, w) are the velocity components in (x, y, z) directions, respectively, n is the kinematic viscosity, T is the temperature of the fluid inside the thermal boundary layer, whereas T_∞ is the ambient temperature, b is the Casson parameter. $u_w(x)$ is the velocity of the stretching surface, b being a positive constant. β is the thermal expansion coefficient and ρ is the density of the fluid. A majority of the existing exact solutions in fluid mechanics are similarity solutions which reduce the number of independent variables by one or more. The methods for generating similarity transformations for equations of physical interest are discussed by Ames [1965]. Similarity solutions are often asymptotic solutions to a given problem and may have utility in this area of limiting solutions. Similarity solutions may be used to gain physical insight into these details of complex fluid flows and these solutions exhibit most of the characteristic as well as the influence of the physical and thermal parameters of the actual problem. In order to get a similarity solution of the problem we define the following transformations:

$$u = bx f'(h) + A\cos q\, M(h),\quad v = A\sin q\, N(h),\quad w = -\sqrt{bn}\, f(h)$$
$$h = \sqrt{\frac{b}{n}}\, z,\quad A = \frac{\beta g (T_w - T_\infty)}{b},\quad H(h) = \frac{T - T_\infty}{T_w - T_\infty} \quad (7)$$

Upon substituting Equation (7) into Equations (2) and (5), we obtain the following ordinary differential equations:

$$\left(\frac{1+b}{b}\right) f''' + f f'' - f'^2 = 0 \quad (8)$$

$$\frac{1}{\Pr} H'' + f H' = 0 \quad (9)$$

$$\left(\frac{1+b}{b}\right) N'' + f N' + H = 0 \quad (10)$$

$$\left(\frac{1+b}{b}\right) M'' + f M' - M f' + H = 0 \quad (11)$$

The boundary conditions (6) can be written as follows

$$f(0) = f_w,\quad f'(0) = 1,\quad H(0) = 1,\quad M(0) = N(0) = 0$$
$$f(\infty) \to 0,\quad H(\infty) \to 0,\quad N(\infty) \to 0,\quad M(\infty) \to 0 \quad (12)$$

In the equations, the prime denotes ordinary differentiation with respect to the similarity variable h, and the mass transfer parameter $f_w = -W\sqrt{bn}$ is negative for injection and positive for suction. The local heat flux may be determined by Fourier's Law as:

$$q_w = -k\left.\frac{\partial T}{\partial z}\right|_{z=0} = -k\sqrt{\frac{b}{n}}(T_w - T_\infty)H'(0)$$

The local heat transfer coefficient is given by:

$$h = \frac{q_w}{T_w - T_\infty}$$

In practical applications, the quantity of physical interest in our case is the local Nusselt number Nu, which may be written in non-dimensional form as:

$$Nu = \frac{hL}{k} = -\sqrt{\mathrm{Re}}\,H'(0) \quad (13)$$

Where $\mathrm{Re} = \frac{bx^2}{n}$ represents Reynolds number. n

In addition, the exact analytical solution of Eq. (8) is given as

$$f(h) = b^{*}\left(1 - e^{-\frac{h}{b^{*}}}\right) - \frac{h}{b^{*}}$$
$$f'(h) = e^{-\frac{h}{b^{*}}},\quad f''(h) = -\frac{1}{b^{*}}e^{-\frac{h}{b^{*}}} \quad (14)$$

With $b^{*} = \sqrt{1 + \frac{1}{b}}$, Now, we can write that if $f(h)$ and its derivatives are given by the exact solution (14), then the temperature distribution $H(h)$ can be solved analytically as:

$$H(h) = \frac{1}{\int_0^\infty e^{-\Pr\int_0^h f\,dh}\,dh}\int_h^\infty e^{-\Pr\int_0^h f\,dh}\,dh$$

Table 1. Comparison values of $f''(0)$, $H'(0)$, $N'(0)$ and $M'(0)$ for various values of Prandtl number when $f_w = 0$ and $b \to \infty$ (Newtonian fluid) [Gorla and Ibrahim, 1994].

Pr	$f''(0)$		$H'(0)$		$N'(0)$		$M'(0)$	
	Gorla, Ibrahim	Present	Gorla, Ibrahim	Present	Gorla, Ibrahim	Present	Gorla, Ibrahim	Present
0.07	-1.01435	-0.99956	-0.06562	-0.10128	8.69012	3.89642	5.74631	2.68875
0.2	-1.01435	-0.99956	-0.16912	-0.17880	3.28714	2.78227	2.30913	1.98471
0.7	-1.01435	-0.99956	-0.53488	-0.45390	0.81521	1.210093	0.69620	0.95644
2.0	-1.01435	-0.99956	-0.91142	-0.91109	0.61602	0.61718	0.52651	0.53413
3.0	-1.01435	-0.99956	-1.15970	-1.16515	0.47431	0.48898	0.42337	0.43525
7.0	-1.01435	-0.99956	-1.89046	-1.89627	0.30942	0.30908	0.28197	0.28870
10	-1.01435	-0.99956	-2.30350	-2.30949	0.25439	0.25669	0.23952	0.24389
20	-1.01435	-0.99956	-3.35391	-3.35674	0.17964	0.18034	0.17045	0.17651
50	-1.01435	-0.99956	-5.42474	-5.43271	0.11281	0.11433	0.10919	0.11603
70	-1.01435	-0.99956	-6.46221	-6.46698	0.09562	0.09693	0.09271	0.09972

Table 2. Comparison values of $f''(0)$, $H'(0)$, $N'(0)$ and $M'(0)$ for various values of mass transfer parameter when $\mathbf{Pr} = 7$ and $b \to \infty$ (Newtonian fluid) [Gorla and Ibrahim, 1994].

f_w	$f''(0)$		$H'(0)$		$N'(0)$		$M'(0)$	
	Gorla, Ibrahim	Present	Gorla, Ibrahim	Present	Gorla, Ibrahim	Present	Gorla, Ibrahim	Present
-0.7	-0.72252	-0.70938	-0.08715	-0.09198	0.69711	0.72849	0.58929	0.59074
-0.4	-0.83420	-0.81968	-0.50012	-0.50768	0.50709	0.52185	0.44702	0.45212
0.0	-1.01435	-0.99954	-1.89046	-1.89627	0.30554	0.30908	0.28197	0.28870
0.4	-1.23180	-1.21870	-3.98932	-3.99699	0.19490	0.19392	0.18525	0.19299
0.7	-1.41884	-1.40775	-5.30002	-5.44026	0.03024	0.14582	0.02741	0.15109

RESULTS AND DISCUSSION

In the present contribution, numerical calculations are performed for the boundary layer flow heat transfer of non-Newtonian Casson fluid past a stretching plane with mass transfer effect. Moreover, the system of ordinary differential equations (8)-(11) subject to the boundary conditions (12) was solved numerically using the function bvp4c from Matlab for different values of the Casson parameter and mass transfer f_w. The Prandtl number $\mathbf{Pr}$ is set equal to 6.2 (water) throughout the paper. The relative tolerance was set to 10^{-10}. In this method, we have chosen a suitable finite value of $h \to \infty$ namely $h = h_\infty = 15$. Since the present problem may have more than one (dual) solution, the bvp4c function requires an initial guess of the desired solution for the ordinary differential Equations (8) to (11). The guess should satisfy the boundary conditions and reveal the behavior of the solution. Determining an initial guess for the first (upper branch) solution is not difficult because the bvp4c method will converge to the first solution even for poor guesses. However, it is difficult to come up with a sufficiently good guess for the solution of the system of the ordinary differential Equations (8) to (11) in the case of opposing flow. To overcome this difficulty, we start with a set of parameter values for which the problem is easy to be solved. Then, we use the obtained result as initial guess for the solution of the problem with small variation of the parameters. This is repeated until the right values of the parameters are reached. The results are given to carry out a parametric study showing influences of several non-dimensional parameters, namely, Casson parameter b, Prandtl number $\mathbf{Pr}$ and mass transfer parameter f_w. For the validation of the numerical results have been obtained in this study, the case when the Casson parameter approaches to infinity ($b \to \infty$, that is Newtonian fluid case) has been considered and compared with the previously published results. Tables 1 and 2 present the numerical values of $f''(0)$, $M'(0)$ and $N'(0)$ with the results reported by Gorla and Ibrahim [1994] which show a very good agreement.

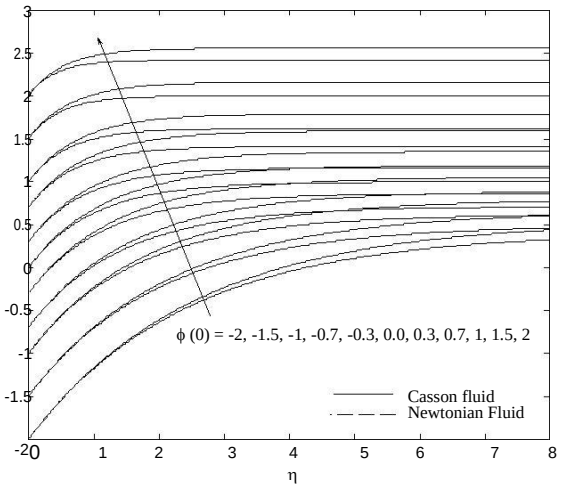

Figure 2. Stream function as a function of the suction or injection parameter.

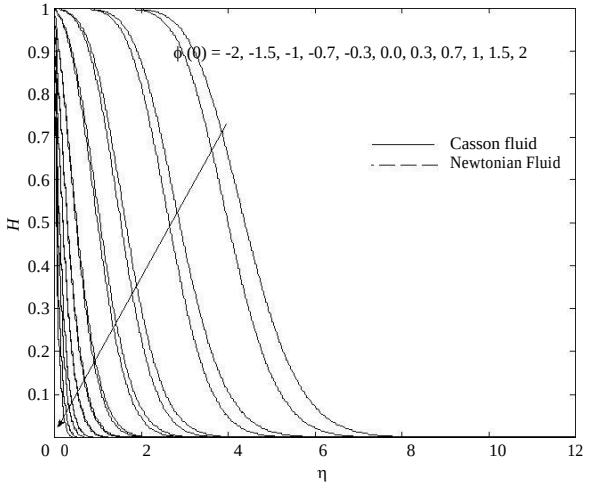

Figure 4. Distribution of temperature H as a function of the suction or injection parameter.

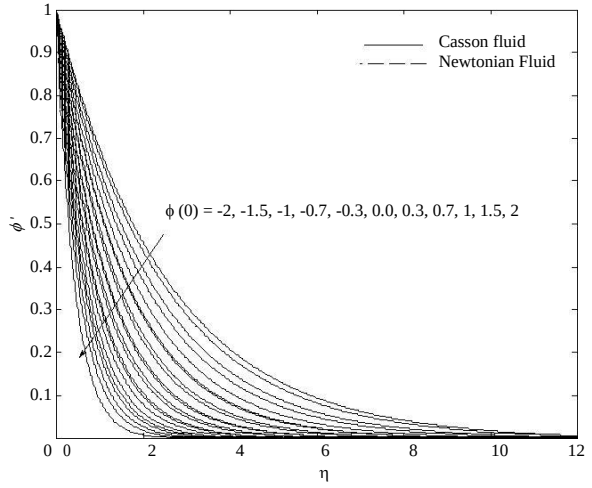

Figure 3. Distribution of f' as a function of the suction or injection parameter.

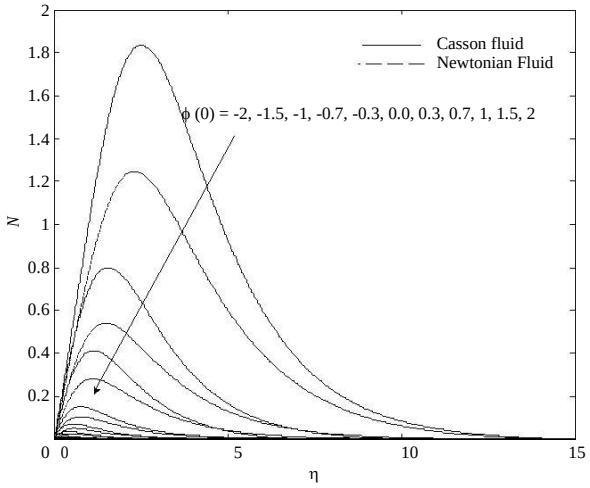

Figure 5. Decay of velocity N as a function of the suction or injection parameter.

Figures 2 to 6 illustrate the effects of surface mass transfer on the velocity and temperature distributions for Newtonian and non-Newtonian Casson fluids. Figure 2 displays the distribution of the velocity component in the z -direction for $\mathbf{Pr = 6.2}$ considering Newtonian and Casson fluid. The surface mass transfer value $f(0)$ has a lot influence on the magnitude of $f(h)$. It is observed that $f(h)$ approaches a constant value $f(\infty)$ monotonically such that $f'(\infty) \to 0$. The values of $f(\infty)$ are found from the numerical solution and are a measure of the entrainment velocity. We notice from Figure 2 that higher entrainment velocities are produced with higher values of suction velocity at the surface. Figure 3 shows the distribution of $f'(h)$ within the boundary layer. It is observed that higher values of injection rates results in more linear shape for $f'(h)$. Figure 4 illustrates the distribution of the normalized temperature profiles for $\mathbf{Pr = 6.2}$ with the surface mass parameter treated as a variable. We observe that high suction at the surface reduces the thermal boundary layer thickness and high injection increases the thermal boundary layer thickness. In all cases, the exponential decay of the thermal boundary layer is evident. Increasing values of injection rates move the location of the maximum $M(h)$ values of (normalized free convection velocity in x -direction) and $N(h)$ (normalized free convection velocity in y -direction)

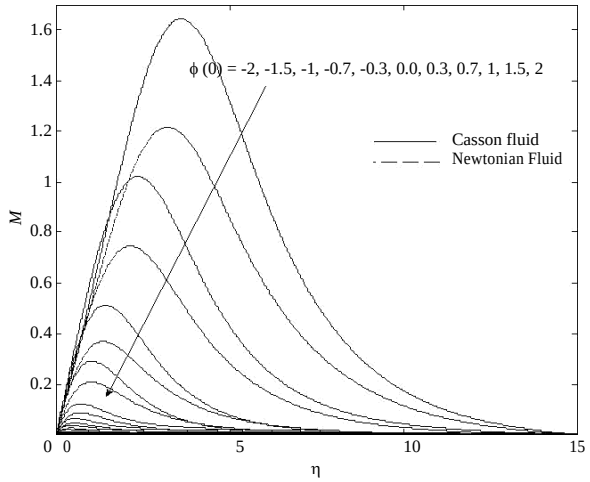

Figure 6. Decay of velocity M as a function of the suction or injection parameter.

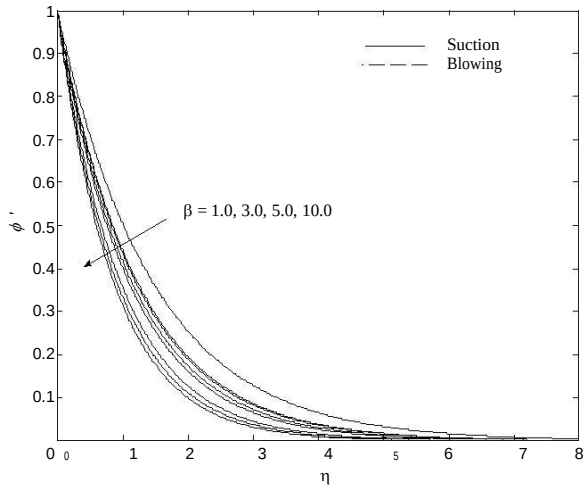

Figure 8. Distribution of f ¢ as a function of Casson parameter.

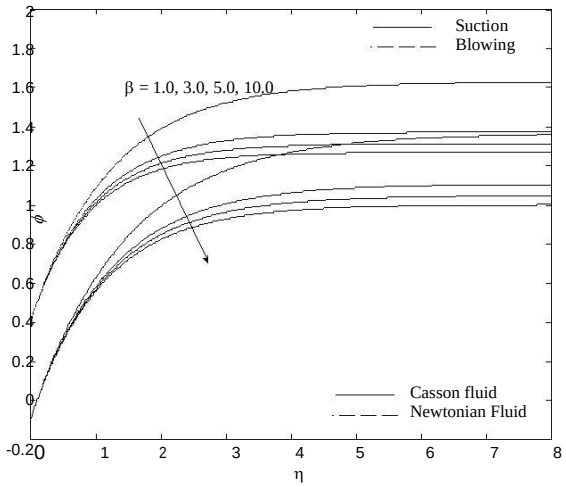

Figure 7. Stream function f as a function of Casson parameter.

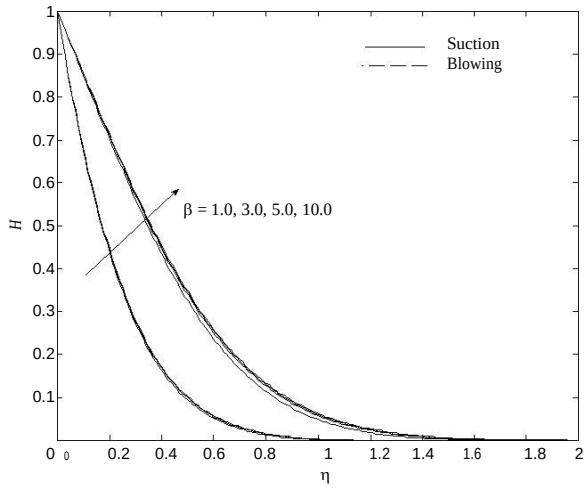

Figure 9. Distribution of temperature H as a function of Casson parameter.

profiles away from the surface. The exponential decay of the velocity boundary layer is evident from the profiles presented (Figures 5 and 6). On the other hand, Figures 7 to 11 depict the influences of non-Newtonian Casson parameter β on temperature and velocity, distributions. The increasing values of the Casson parameter that is the decreasing yield stress (the fluid behaves as Newtonian fluid as Casson parameter becomes large) suppress the velocity field. The effect of increasing values of β is to reduce the rate of transport, and hence, the boundary layer thickness decreases. It is observed that $f(h)$, f ¢(h) and the associated boundary layer thickness are decreasing function of β, whereas, both of $M(h)$ and $N(h)$ increase with increasing Casson parameter. The effect of increasing β leads to enhance the temperature profile $H(h)$ as seen from Figure 9. The thickening of the thermal boundary layer occurs due to increase in the elasticity stress parameter. Prandtl number signifies the ratio of momentum diffusivity to thermal diffusivity. It is seen that the temperature decreases with increasing $\mathbf{Pr}$ as observed from Figure 12. Furthermore, the thermal boundary layer thickness decreases sharply by increasing Prandtl number. The temperature gradient at surface is negative for all values of Prandtl number as seen from Figure 13 which means that the heat is always transferred from the surface to the ambient fluid. Fluids with lower Prandtl number will possess higher thermal conductivities (and thicker

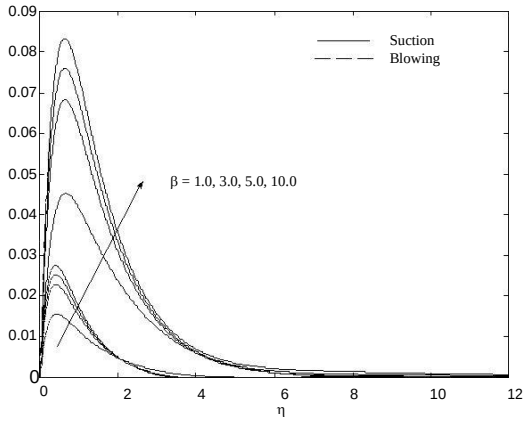

Figure 10. Decay of velocity N as a function of Casson parameter.

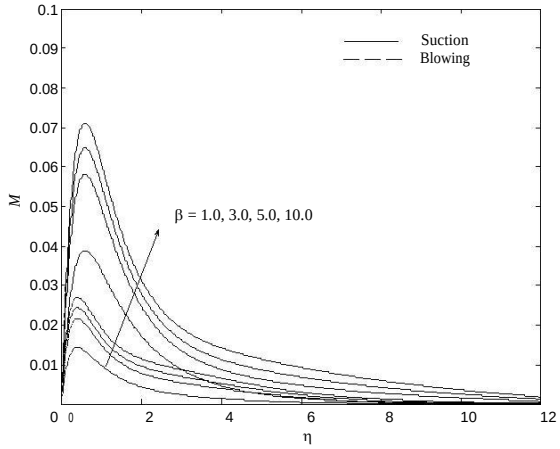

Figure 11. Decay of velocity M as a function of Casson parameter.

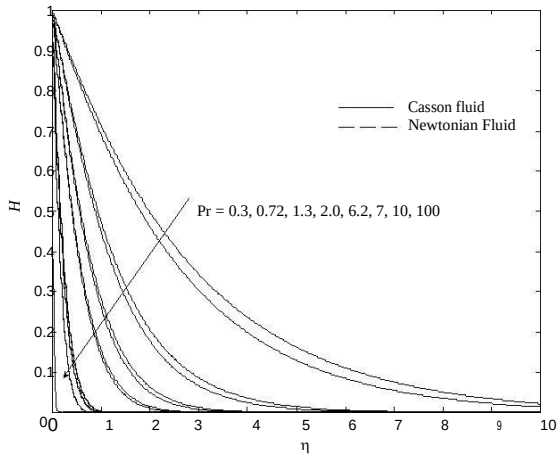

Figure 12. Distribution of temperature H as a function of Prandtl number.

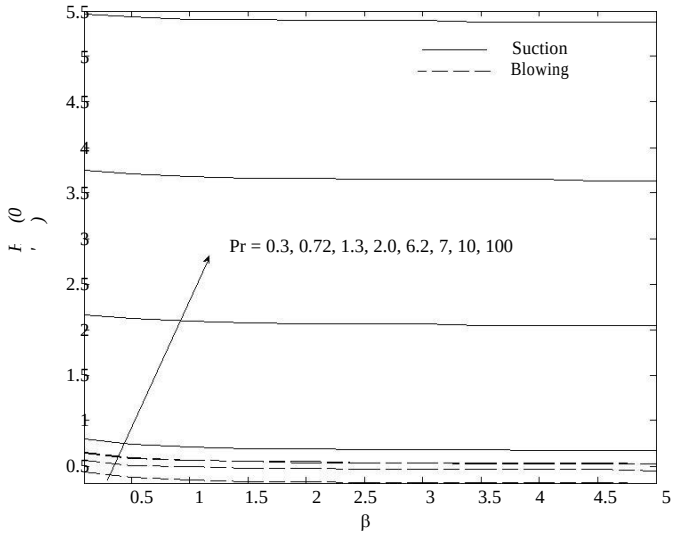

Figure 13. Temperature gradient - H ¢(0) as a function of Casson parameter with different values of Prandtl number.

thermal boundary layer structures), so that heat can diffuse from the surface faster than for higher **Pr** fluids (thinner boundary layers). Physically, if **Pr** increases, the thermal diffusivity decreases and this phenomenon leads to decrease the energy transfer ability and reduces the thermal boundary layer. In addition, Figures 14 to 16 display the effect of mass transfer parameter and it is observed that an increase in mass transfer parameter tends to decrease all f ¢¢(0), M ¢(0) and N ¢(0) .

Conclusions

A numerical study of natural convection, steady three dimensional boundary layer flow and heat transfer of non-Newtonian Casson fluid over a stretching sheet with suction or injection effect has been performed. It is shown in this paper how the Prandtl number **Pr** , and Casson parameter affect the temperature distribution, velocity and the heat transfer coefficient. We can conclude that:

- The effect of increasing values of the Casson parameter b is to suppress the velocity field, whereas the temperature is enhanced with increasing Casson parameter.
- The thermal boundary layer thickness depends strongly on the Prandtl number **Pr** . Further; it is found that an increase in **Pr** results in a decrease of the temperature distribution and thermal boundary layer thickness.
- Surface mass transfer rate influences the flow and temperature fields. Suction at the surface produces higher entrainment velocities, whereas injection makes the velocity and temperature distributions more linear.

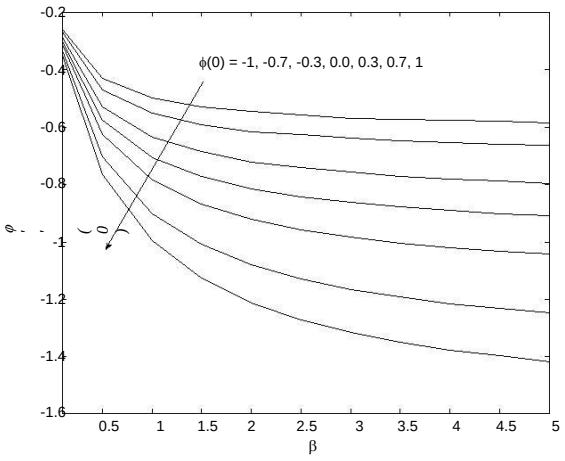

Figure 14. Variation of $f''(0)$ as a function of Casson parameter for various suction or injection parameters.

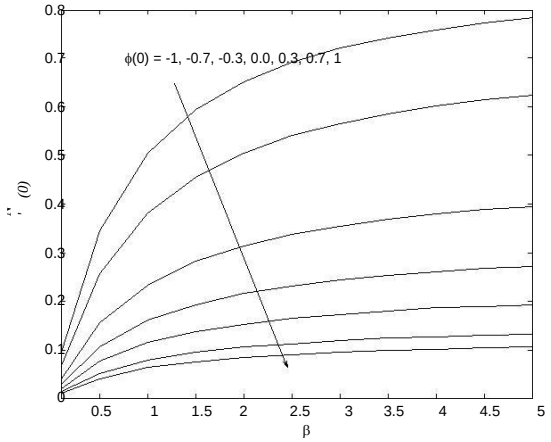

Figure 15. Variation of $N'(0)$ as a function of Casson parameter for various suction or injection parameters.

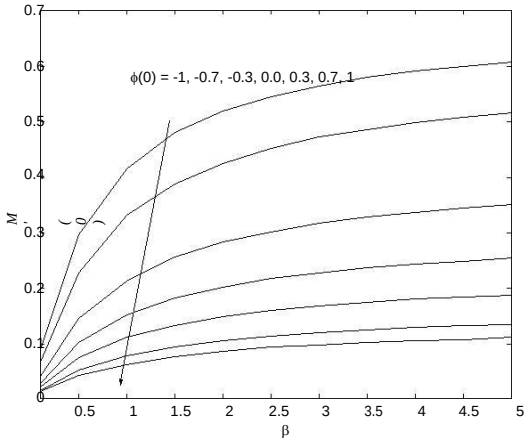

Figure 16. Variation of $M'(0)$ as a function of Casson parameter for various suction or injection parameters.

- Surface suction reduces the thermal boundary layer thickness while injection increases it.

REFERENCES

Ames WF (1965) Nonlinear partial differential equations, New York, Academic Press.

Banks WHH (1983) Similarity solutions of the boundary-layer equations for a stretching wall. J Mech Theor Appl 2: 375–392.

Bird RB, Stewart WE, Lightfoot EN (1960) Transport Phenomena, Wiley, New York 94–95, 104–105.

Boyd J, Buick J, Green MS (2007) Analysis of the Casson and CarreauYasuda non-Newtonian blood models in steady and oscillatory flow using the lattice Boltzmann method. Phys Fluids 19: 93–103.

Casson N in: C. C. Mills (Ed.) (1959) Rheology of Disperse Systems, Pergamon, New York (1959) Ch. 5.

Chevalley J (1991) An adaptation of the Casson equation for the rheology of chocolate. J Texture Stud 22: 219–229.

Churchill SW (1988) Viscous Flows: The Practical Use of Theory, Butterworths, Boston Ch. 5.

Cokelet GR, et al. (1963) The rheology of human blood—measurement near and at zero shear rate. Trans Soc Rheol 7: 303–317.

Crane LJ (1970) Flow past a stretching plate. J Appl Math Phys (ZAMP) 21: 645–647.

Eldabe NTM, Salwa MGE (1995) Heat transfer of MHD non-Newtonian Casson fluid flow between two rotating cylinder. J Phys Soc Jpn 64: 41–64.

Fung YC (1981) Biomechanics, Mechanical properties of living tissues, Chap 3. Springer-Verlag, New York.

Garcia-Ochoa F, Casas JA (1994) Apparent yield stress in xanthan gum solutions at low concentrations. Chem Eng J 53: B41–B46.

Gorla RSR, Ibrahim S (1994) Free convection on a vertical stretching surface with suction and blowing, Appl Sci Res 52: 247-257.

Grubka IJ, Bobba KM (1985) Heat transfer characteristics of a continuous stretching surface with variable temperature. ASME J Heat Transfer 107: 248–250.

Joye DD (1998) in: Hazardous and Industrial Wastes Proc. 30th Mid-Atlantic Industrial Waste Conf Technomic Publ. Corp. Lancaster PA/Basel 567–575.

Kirsanov EA, Remizov SV (1999) Application of the Casson model to thixotropic waxy crude oil. Rheol Acta 38: 172–176.

Kumari SVHNK, Murthy MVR, Reddy MCK, Kumar YVKR (2011) Peristaltic pumping of a magnetohydrodynamic Casson fluid in an inclined channel. Adv Appl Sci Res 2: 428–436.

Liao S, Pop I (2004) On explicit analytic solutions of boundary-layer equations about flows in a porous medium or for a stretching wall. Int J Heat Mass Transf

47: 5–85.

Magyari E, Keller B (2000). Exact solutions for self-similar boundary-layer flows induced by permeable stretching walls. Eur J Mech B/Fluids 19: 109–122.

Nadeem S, Haq RU, Akbar NS (2014a). MHD three dimensional boundary layer flow of Casson nanofluid past a linearly Stretching sheet with convective boundary condition. IEEE Transactions Nanotechnology 13: 109-115.

Nadeem S, Haq RU, Lee C (2012) MHD flow of a Casson fluid over an exponentially shrinking sheet. Scientia Iranica 19: 1550–1553.

Nadeem S, Rizwan Ul Haq, Noreen Sher Akbar, Z.H. Khan (2013). MHD three dimensional flow of Casson fluid past a porous linearly Stretching sheet, Alexandria Engineering J., 52: 577–582.

Nadeem S, Mehmood Rashid, Noreen Sher Akbar (2014b). Optimized analytical solution for oblique flow of a Casson-nano fluid with convective boundary conditions. Int. J. Thermal Sciences. 78: 90-100.

Nadeem S, Mehmood Rashid, Akbar Noreen Sher (201c). Oblique stagnation point flow of a Casson-Nano fluid towards a stretching surface with heat transfer. J. Computational Theoretical Nanosciences, 11: 1422-1432.

Oka S (1979) Festschrift of Harold Wayland Symposium, California Inst. of Tech., Pasadena.

Reher EO, Haroske D, Kohler K (1969) Chem Technol 21: 137– 143.

Swati Mukhopadhyay, Prativa Ranjan De, Krishnendu Bhattacharyya, Layek GC (2013) Casson fluid flow over an unsteady stretching surface. Ain Shams Eng J 4: 933-938.

Wilkinson WL (1960) Non-Newtonian Fluids, Pergamon, New York, (1960).

Nomenclature

A	Free convection parameter
b	Positive constant
H	Dimensionless temperature
k	Thermal conductivity
M	Dimensionless in x -direction
N	Dimensionless in y -direction
Nu	Nusselt number
$\mathbf{Pr}$	Prandtl number
q_w	Surface heat flux
$\mathbf{Re}$	Reynolds number
T	Temperature of the fluid
(u, v, w)	Velocity components of the fluid
u_w	Velocity of stretching sheet
(x, y, z)	Coordinate axes

Greek symbols

f	Dimensionless velocity
b^*	Casson parameter
b	Thermal expansion coefficient
q	Angle
n	Kinematic viscosity
h	Similarity variable

Subscripts

w	Conditions at the surface of cylinder
¥	Conditions in the free stream